

An Active Contour Model for Silhouette Vectorization using Bézier Curves

Luis Alvarez^{1*} and Jean-Michel Morel^{2†}

^{1*}Departamento de Informática y Sistemas, Universidad de Las Palmas de Gran Canaria, Campus de Tafira, Las Palmas de G.C., 35017, Spain.

²Department of Mathematics, City University of Hong Kong, Tat Chee Avenue, Kowloon Tong, Hong Kong.

*Corresponding author(s). E-mail(s): lalvarez@ulpgc.es;

Contributing authors: jeamorel@cityu.edu.hk;

†These authors contributed equally to this work.

Abstract

In this paper, we propose an active contour model for silhouette vectorization using cubic Bézier curves. Among the end points of the Bézier curves, we distinguish between corner and regular points where the orientation of the tangent vector is prescribed. By minimizing the distance of the Bézier curves to the silhouette boundary, the active contour model optimizes the location of the Bézier curves end points, the orientation of the tangent vectors in the regular points, and the estimation of the Bézier curve parameters. This active contour model can use the silhouette vectorization obtained by any method as an initial guess. The proposed method significantly reduces the average distance between the silhouette boundary and its vectorization obtained by the world-class graphic software Inkscape, Adobe Illustrator, and a curvature-based vectorization method, which we introduce for comparison. Our method also allows us to impose additional regularity on the Bézier curves by reducing their lengths.

Keywords: Silhouette vectorization, image tracing, active contours, Bézier curves

1 Introduction

Most digital images are acquired as a raster image, defined by values on a regular grid of pixels. When the image is binary, the shapes that are observed in the image appear as unions of square pixels. This pixel representation, viewed as a subset of the plane, has a very weak structure. For example, most boundary pixels add artificial corners to the shape, a phenomenon known as the pixelation effect [1]. The shape cannot be directly

rescaled, translated, rotated, etc. without accentuating these defects[2–4]. Silhouette vectorization (also called silhouette tracing) is a process in which the outline or silhouette of an object in an image is extracted and represented as a vector graphic. Vectorization involves converting binary raster shapes, which are simply unions of pixels, into a vector graphics representation where the shape boundary is described by mathematical equations (usually cubic Bézier curves). Silhouette vectorization is particularly useful in various applications, including graphic design, computer

vision, and image processing. The main steps involved in silhouette vectorization are usually:

1. Decomposition of the silhouette boundary as a collection of closed curves.
2. For each closed curve, $C(t)$, selection of a subset of points $\{C(t_n) = \bar{x}_n\}$ that are the end points of the cubic Bézier curves used to approximate the silhouette boundary.
3. Estimation of the parameters of the cubic Bézier curves approximating $C(t)$.

Among the Bézier curve end points we can distinguish between corner points, where the boundary curves ending at the point change direction, and regular points, where the curves have a prescribed tangent vector orientation. We denote by $Corners \subset \{t_n\}$, the set of corner points. In this paper, we propose an active contour model that fits the cubic Bézier curves to $C(t)$ by optimizing the choice of the interpolating values t_n , the orientation of the tangent vectors at the regular points, and the Bézier curve parameters. This active contour model is based on minimization of the distance of the Bézier curves to the silhouette boundary. The main contributions of the paper are:

1. The formulation of the active contour model optimizing the approximation of the silhouette boundary by a collection of cubic Bézier curves.
2. The representation, in the active contour model, of the control points of the Bézier curves in terms of the tangent vectors at the end points, which makes it easy to constrain the value of the tangent vectors at the regular points.
3. The active contour model optimizes not only the position of the control points of the Bézier curves, but also the positions of their end points and the orientation of the tangent vectors at the regular points.
4. The method can be used to improve the results obtained by any vectorization method. In particular, we show that it significantly reduces the average distance between the silhouette boundary and its vectorization obtained by Inkscape, Adobe Illustrator and a basic curvature-based vectorization method that we introduce for comparison purposes.
5. The proposed active contour model also allows for imposing additional regularity on the Bézier

curves to remove, if needed, undesirable irregularities.

2 Related work

Image vectorization and its advantages

Image vectorization is a technique to transform a raster image into an image that avoids pixelation defects by representing the image by a finite number of smooth curves that separate regions endowed with a constant or parametric color model. This *vector graphic* representation is highly successful [5, 6]. Image vectorization gives a grid-invariant representation [7–9], enabling content editing [10], the reconstruction of line drawings and cartoons [11–14], and clipart [15, 16]. In most vectorized images [17–20] the image regions are encoded by a parametric color description, often simply a constant color in each region, separated by curves composed of Bézier curves. These parametric curves have precise grid-independent shapes that justify their name of Scalable Vector Graphic (SVG) [21]. When displayed on a screen or printed, such images must be converted back to raster images. This rendering process reverses the vectorization process and simulates optical blur using so-called anti-aliasing filters. All graphic software [22] enables this instant conversion at any required image scale. Note that more advanced vector graphic representations than SVG have been proposed involving mesh generation [23] and elliptic equations used as interpolators [10]. Recent deep learning methods that optimize the shape and color control points of deformable objects have also been proposed [20, 24–26]. In the context of silhouette vectorization, cubic Bézier curves are often used to represent smooth and precise curves defining the silhouette boundary. The control points of the Bézier curves are adjusted to match the shape of the extracted contours. There exist many different ways to fit the curve C by cubic Bézier curves (see, for instance, [27]). The open source Inkscape [28] trace bitmap tool performs silhouette vectorization based on a polygonal approximation of the silhouette boundary and cubic Bézier curves. In [29], the authors use Bézier curves including a parameter controlling the complexity and resolution of the approximation process. In [30] the authors use Bézier curves with tangent vector

specifications. In [31] the authors use the affine scale-space to select the end points of the Bézier curves. In [32] the authors propose a method for vectorization of color images.

Variational models of shape approximation, curve shortening models

Starting as early as 1972 variational image segmentation [33] models led to the general *Mumford-Shah functional* [34, 35]:

$$\mathcal{E}_f(u, \Gamma) = \int_{\Omega \setminus \Gamma} \|u(x) - f(x)\|_2^2 dx + \int_{\Omega \setminus \Gamma} \|\nabla u(x)\|_2^2 dx + \lambda \int_{\Gamma} d\sigma(x). \quad (1)$$

The reconstructed image $u : \Omega \rightarrow \mathbb{R}^d$ ($d = 1$ or 3) is obtained as an approximation of the input image $f : \Omega \rightarrow \mathbb{R}^d$. In (1), $\Gamma \subset \mathbb{R}^2$ is the discontinuity set of u , $\lambda > 0$ is the regularization parameter, and $d\sigma$ is the length element. The pair (u, Γ) can be understood as a set of smooth regions whose smoothness is controlled in the second term, separated by curves whose smoothness is enforced by minimizing the length in the third term. Variational segmentation models such as (1) are non-convex and non-smooth optimization problems [36, 37] that require a sophisticated optimization machinery [38–40]. The application to the approximation of a single shape in an image is the celebrated snakes model [41] which introduced the notion of active contour models minimizing again a functional where the smoothness of the contour competes with its fidelity to the image’s discontinuities. The complexity of its optimization has led to a rich literature [42, 43, 43–46].

Curve smoothing and curve shortening

Bounded shapes in the plane can be modeled as Caccioppoli sets [47]. Their boundary is a union of nested Jordan curves [48]. When this boundary is a simple curve, we call the shape a silhouette. Smoothing the shape then amounts to smoothing this simple curve. The curve shortening flow, or evolution of a simple curve by the intrinsic heat equation, was shown in [49] to be a consistent model that progressively reduces the complexity of the curve until it collapses at a round point [50]. It can be viewed as the unconstrained gradient

descent of the third term of the Mumford-Shah functional. As anticipated in [51], the analysis of a curve focuses on its extrema of curvature [52]. The curve shortening flow is often interpreted as a *motion by curvature* [53] because, in the shortening flow, the points of the curve move with a velocity proportional to their curvature. An important variant is the affine curve shortening flow, which has very similar properties, but also commutes with affine perspective deformations, a desirable property in shape analysis [54–56]. There is a very fast consistent scheme [57] for this curve evolution, which is used in [17, 58] for shape vectorization. The method [59] develops an extension of the silhouette affine shortening to general image vectorization, and a variant [9] focuses on evolving the curves that support T-junctions. The affine curve shortening flow has also been shown to be very efficient for the multiscale detection of curve corners [60, 61] and of multiple junctions. See also [62] for the curvature motion of planar graphs.

In the seminal paper [63], Caselles et al. introduced the geodesic active contour formulation given by

$$\mathcal{E}(B) \equiv \int_0^1 g(B(s)) \|B'(s)\| ds, \quad (2)$$

where $B : [0, 1] \rightarrow \mathbb{R}^2$. $\mathcal{E}(B)$ corresponds to a curve length definition obtained by weighting the Euclidean element of length $\|B'(s)\| ds$ by $g(B(s))$. This simple and elegant formulation has been successfully applied to many different scenarios. Geodesic contours model with prior shapes information have been formulated in [64] and [65] using a level set evolution approach where the evolving curve is represented as the boundary of the zero level set of an evolving surface. In [66], it has also been applied to the regularization of 3D curves using as function $g(\bar{x})$:

$$g(\bar{x}) = d_C(\bar{x}) + w, \quad (3)$$

where $d_C(\bar{x})$ is the Euclidean distance of any 3D point \bar{x} to a prescribed curve $C : [0, T] \rightarrow \mathbb{R}^3$ and $w \geq 0$. For this choice of $g(\bar{x})$, the minimization of (2) yields a curve close to $C(t)$. The parameter w is a regularization factor that penalizes large values of the length of $B(s)$ in the energy.

The active contour model that we propose in this paper is based on the geodesic active contour (2) with $g(\bar{x})$ given by (3) (but in R^2 and with $C(t)$ a closed curve on the silhouette boundary). In our case, the curve $B(s)$ is parameterized using a collection of cubic Bézier curves with prescribed tangent orientation in the regular points. Parameterized active contours have been used, for instance, for the detection and tracking of circles [67], and ellipses [68]. Using parameterized active contours simplifies the minimization of energy (2) and, in general, we can use $w = 0$ as a regularization parameter, because the parameterized curves used are, in general, smooth.

3 The active contour model

The input of the active contour model we propose is given by :

1. A closed curve $C : [0, T] \rightarrow R^2$.
2. An initial collection of interpolating values $\{t_n\}_{n=1, \dots, N}$ with $0 \leq t_1 < t_2 < \dots < t_N < T$, with the associated 2D points $\bar{x}_n = C(t_n)$. As we deal with closed curves, to simplify the presentation, we consider that the position $N+1$ is identified with the first position, that is $t_{N+1} = t_1$. For any $t, t' \in [0, T]$ with $t' < t$, we consider that $[t, t'] = [t, T] \cup [0, t']$. We denote by L_n the length of $C(t)$ between t_n and t_{n+1} .
3. The set of corner points $Corners \subset \{t_n\}$ where no restriction is imposed about the Bézier curve parameters.
4. $\mathcal{T}(\alpha_n) = (\cos(\alpha_n), \sin(\alpha_n))^T$ the initial unit tangent vectors to $C(t)$ at t_n and $\mathcal{T}(\alpha_n)^\perp = (-\sin(\alpha_n), \cos(\alpha_n))^T$ their orthogonal direction. In the regular points, $t_n \notin Corners$, we constrain the tangent vector of the Bézier curve to be aligned with $\mathcal{T}(\alpha_n)$.

We define the cubic Bézier curve $B_n : [0, L_n] \rightarrow R^2$, which approximates $C(t)$ in the interval $[t_n, t_{n+1}]$ by

$$B_n(s) = \left(1 - \frac{s}{L_n}\right)^3 \bar{x}_n + 3\left(1 - \frac{s}{L_n}\right)^2 \frac{s}{L_n} (\bar{x}_n + \lambda_n L_n \mathcal{T}(\alpha_n) + \gamma_n L_n \mathcal{T}(\alpha_n)^\perp) + 3\left(1 - \frac{s}{L_n}\right) \left(\frac{s}{L_n}\right)^2 (\bar{x}_{n+1} - \beta_n L_n \mathcal{T}(\alpha_{n+1}) -$$

$$\delta_n L_n \mathcal{T}(\alpha_{n+1})^\perp) + \left(\frac{s}{L_n}\right)^3 \bar{x}_{n+1}, \quad (4)$$

where the parameters $\lambda_n, \gamma_n, \beta_n, \delta_n \in R$ determine the Bézier curve control points. $B_n(s)$ satisfies:

$$\begin{aligned} B_n(0) &= \bar{x}_n, \\ B'_n(0) &= 3(\lambda_n \mathcal{T}(\alpha_n) + \gamma_n \mathcal{T}(\alpha_n)^\perp) \\ B_{n-1}(L_{n-1}) &= \bar{x}_n, \\ B'_{n-1}(L_{n-1}) &= 3(\beta_{n-1} \mathcal{T}(\alpha_n) + \delta_{n-1} \mathcal{T}(\alpha_n)^\perp). \end{aligned} \quad (5)$$

In this formulation of the cubic Bézier curve, the tangent vector at the end points is expressed in the local reference system given by $\mathcal{T}(\alpha_n)$ and $\mathcal{T}(\alpha_n)^\perp$. We assume that in the regular points ($t_n \notin Corners$), $\gamma_n = \delta_{n-1} = 0$ which means that at \bar{x}_n , the tangent vectors to $B_{n-1}(s)$ and to $B_n(s)$ are aligned with $\mathcal{T}(\alpha_n)$. In the corner points, the Bézier curve parameters are completely free, in particular, in this case, the choice of α_n does not affect the final result because we can obtain any configuration of the Bézier curve control points independently of the value of α_n .

The active contour model we propose to fit the Bézier curves to $C(t)$ is given by the adjustment error functional

$$\mathcal{E}(\{t_n, \alpha_n, \lambda_n, \gamma_n, \beta_n, \delta_n\}_{n=1}^N) := \sum_{n=1}^N \int_0^{L_n} (d_C(B_n(s)) + w_n) \|B'_n(s)\| ds, \quad (6)$$

where $d_C : R^2 \rightarrow R^+$ is the Euclidean distance from any point $\bar{x} \in R^2$ to $C(t)$ and $w_n \geq 0$. By minimizing this functional, we look for a Bézier curve collection with minimal distance to $C(t)$ among all Bézier curves. The weight parameter $w_n \geq 0$ optionally introduces an additional regularization by penalizing the length of $B_n(s)$. In our experiments, we always initially fix $w_n \equiv 0$, which in general provides good results, and optionally increase the value of w_n to remove the undesirable irregularities that can appear in particular Bézier sections $B_n(s)$ of the curve. Notice that minimization is constrained by the conditions $\gamma_n = \delta_{n-1} = 0$ for $t_n \notin Corners$. The main advantages of this active contour model are :

1. The model enables simultaneous optimization of the location of the interpolation values t_n , the orientation of the vectors tangent to the

curve in the regular points, and the Bézier curve parameters.

2. The explicit introduction, in the Bézier curve representation, of the tangent vectors $\mathcal{T}(\alpha_n)$ at the points \bar{x}_n allows one to manage in a very simple way the orientation of the tangent vectors at the regular points. Indeed, we only have to fix $\gamma_n = \delta_{n-1} = 0$ at the regular points. Moreover, the optimization problem is simplified because we reduce the number of unknowns.
3. If we fix the values of t_n and α_n , the minimization of (6) to estimate the Bézier curve parameters can be performed independently in each interval $[t_n, t_{n+1}]$, which strongly simplifies the complexity of the minimization problem. Moreover, it allows for a simple minimization method, where we alternately optimize the Bézier curve parameters $\alpha_n, \lambda_n, \gamma_n, \beta_n, \delta_n$ and the values t_n and α_n .
4. Given that we always initialize with $w_n = 0$, the management of w_n is an optional post-processing of the Bézier curves.

4 Minimization of the adjustment error functional (6)

First, we highlight that to apply our proposed active contour model, we can use any vectorization method to select the initial collection of Bézier curves. If the method does not provide information about the set of corner points, we can introduce such information by hand or simply define all interpolation points as corners.

For $t, t' \in [0, T]$ we denote by $|C_{t,t'}|$ the length of the curve between t and t' given by

$$|C_{t,t'}| = \int_t^{t'} \|C'(t)\| dt.$$

Let us denote by $B_{t,t',\alpha,\alpha'}(s)$ the Bézier curve with end points $C(t)$ and $C(t')$ and with tangent orientation angles α and α' (in particular we have that $B_n(s) = B_{t_n, t_{n+1}, \alpha_n, \alpha_{n+1}}(s)$). For fixed values of t, t', α, α' , we obtain the Bézier curve parameters by applying a gradient descent method to the functional:

$$E_{t,t',\alpha,\alpha',w}(\lambda, \gamma, \beta, \delta) =$$

$$\int_0^{|C_{t,t'}|} (d_C(B_{t,t',\alpha,\alpha'}(s)) + w) \|B'_{t,t',\alpha,\alpha'}(s)\| ds. \quad (7)$$

As initial guess for the active contour model, we use a linear estimate of the Bézier curve parameters obtained by minimizing the quadratic error

$$Q(\lambda, \gamma, \beta, \delta) = \int_0^{|C_{t,t'}|} \|B_{t,t',\alpha,\alpha'}(|C_{t,s}|) - C(s)\|^2 ds. \quad (8)$$

One can easily show (see, for instance [31]), that the minimization of this quadratic error leads to a linear system of equations. The constraints $\gamma = 0$ if t is a regular point or $\delta = 0$ if t' is a regular point are directly included in the linear estimation of the parameters and in the gradient descent. To compute the distance function $d_C(\bar{x})$ we use an efficient algorithm presented in [69].

To minimize (6) with respect to $\{t_n\}$ and $\{\alpha_n\}$, first we take into account that if $t_{n-1}, t_{n+1}, \alpha_{n-1}$ and α_{n+1} are fixed, we can find the optimal values for t_n and α_n by minimizing the functional :

$$E_n(t, \alpha) = E_{t_{n-1}, t, \alpha_{n-1}, \alpha, w_{n-1}}(\lambda, \gamma, \beta, \delta) + E_{t, t_{n+1}, \alpha, \alpha_{n+1}, w_n}(\lambda, \gamma, \beta, \delta), \quad (9)$$

where for each choice of t and α , the values of $\lambda, \gamma, \beta, \delta$ are, in each case, the one obtained minimizing (7). Therefore, the minimization of (6) can be obtained by iterations based on the following steps:

1. For each $n = 1, \dots, N$:
 - we update $t_n = t_{min}$ and $\alpha_n = \alpha_{min}$ where $(t_{min}, \alpha_{min}) = \arg \min E_n(t, \alpha)$ for $(t, \alpha) \in [t_n - 2, t_n + 2] \times [\alpha_n - r_\alpha, \alpha_n + r_\alpha]$ where r_α is fixed to 4 degrees (in the case of corner points we do not minimize with respect to α).
2. If after updating $\{t_n\}$ and $\{\alpha_n\}$ the functional (6) is significantly reduced, we repeat the previous step to update these values again; otherwise, we stop the iteration.

5 Experiments

For comparison purposes, in addition to the standard vectorization algorithms provided by Inkscape and Adobe Illustrator we also use a

basic vectorization algorithm that we name "curvature method", presented in the Appendix, based on the curvature of the silhouette contour. This basic method allows us to compare the usual linear method (8) to estimate the parameters of the Bézier curves and its improvement using the proposed active contour model.

For simplicity, we make experiments with silhouette contours given by a single Jordan curve $C : [0, T] \rightarrow R^2$. In the case of multiple Jordan curves, we would apply the active contour model independently to each Jordan curve. We denote by $\mathcal{B} = \{B_n(s) : [0, L_n] \rightarrow R^2\}$ the approximation of C by a collection of Bézier curves. To measure the quality of this approximation, we use the average distance between \mathcal{B} and C given by

$$d(\mathcal{B}, C) = \frac{\sum_n \int_0^{L_n} d_C(B_n(s)) \left\| \frac{d}{ds} B_n(s) \right\| ds}{\sum_n \int_0^{L_n} \left\| \frac{d}{ds} B_n(s) \right\| ds}, \quad (10)$$

and the average distance between C and \mathcal{B} given by:

$$d(C, \mathcal{B}) = \frac{\int_0^T d_{\mathcal{B}}(C(t)) \left\| \frac{d}{dt} C(t) \right\| dt}{\int_0^T \left\| \frac{d}{dt} C(t) \right\| dt}. \quad (11)$$

It is very important to check the values of both distances, because it could happen that the Bézier curves \mathcal{B} are close to C ($d(\mathcal{B}, C)$ is small) but that \mathcal{B} does not adequately cover C (that is, $d(C, \mathcal{B})$ is large). The distance $d(\mathcal{B}, C)$ is closely related to the proposed active contour model because our method aims at optimizing the Bézier curves by minimizing the term in the numerator of (10). Notice that it would be possible to use a more symmetric active contour formulation using the combined energy:

$$E(\mathcal{B}) = \int_0^T d_{\mathcal{B}}(C(t)) \left\| \frac{d}{dt} C(t) \right\| dt + \sum_n \int_0^{L_n} d_C(B_n(s)) \left\| \frac{d}{ds} B_n(s) \right\| ds. \quad (12)$$

The main technical limitation of this approach is that each evaluation of $E(\mathcal{B})$ requires the computation of the distance function $d_{\mathcal{B}}(\bar{x})$. Given that minimization of $E(\mathcal{B})$ requires a very large number of evaluations of $E(\mathcal{B})$ for different choices of \mathcal{B} , the computational cost of the algorithm

would be very high. However, as we show in the experiments, with the proposed active contour model, the values obtained for $d(\mathcal{B}, C)$ and $d(C, \mathcal{B})$ are reasonably similar.

We denote by \mathcal{B}_{κ}^0 the initial Bézier curves obtained by the basic curvature based vectorization algorithm presented in the appendix using the linear method (8) to compute the Bézier curves parameters, and by $\mathcal{B}_{\kappa}^{\infty}$ the Bézier curves obtained as the asymptotic state of the active contour model using as initial guess \mathcal{B}_{κ}^0 , by comparing $d(\mathcal{B}_{\kappa}^0, C)$ with $d(\mathcal{B}_{\kappa}^{\infty}, C)$ or $d(C, \mathcal{B}_{\kappa}^0)$ with $d(C, \mathcal{B}_{\kappa}^{\infty})$ we measure the ability of the active contour model to improve the quality of the approximation of the silhouette contour by the Bézier curves obtained using the usual linear method (8) to compute the Bézier curve parameters.

Inkscape is a powerful open source vector graphics editor widely used for creating and editing vector illustrations, logos, icons, diagrams, and complex designs. We use the Inkscape vectorization algorithm (see [28]) to provide the initial guess of our active contour model. In all experiments, we use the Inkscape interface to obtain the silhouette vectorization using the maximum optimization value allowed, then simplify the collection of Bézier curves; we export the result as an SVG file and we read this file to get the initial Bézier curves that we name \mathcal{B}_I^0 . We denote by \mathcal{B}_I^{∞} the asymptotic state of the active contour model using as an initial guess the original Inkscape vectorization \mathcal{B}_I^0 .

Adobe Illustrator is a widely used professional graphic editor. We used the Adobe Illustrator image trace tool to vectorize the image silhouettes we use in our experiments, and we used the Adobe Illustrator simplification tool to reduce the number of end points of the Bézier curves. We denote by \mathcal{B}_A^{∞} the asymptotic state of the active contour model using as initial guess \mathcal{B}_A^0 (the original Adobe Illustrator vectorization).

In the Inkscape and Adobe Illustrator SVG file outputs, we have no information about corner/regular points, so we assume that all points have two half-tangents and, therefore, are "corners".

Our main goal in the experiments is to check if the active contour model is able to significantly reduce the values of $d(\mathcal{B}^0, C)$ and $d(C, \mathcal{B}^0)$. In table 1, we present the results obtained for three silhouettes. Each silhouette is given by a

1024×1024 image. In all experiments, we observe a significant reduction in the distances between $C(t)$ and the Bézier curves before and after applying the proposed active contour model. Notice that the number of nodes (end points) of the Bézier curves can be different among the vectorization methods but we emphasize that for our purpose it is not relevant because we are interested in the ability of the active contour models to reduce the distance between the silhouette contour and the Bézier curves for a given vectorization method.

In Figs. 1, 2 and 3 we show the silhouettes we use in our experiments and the asymptotic state of the active contour model for the different vectorization methods. We highlight that the collection of Bézier curves end-points is very different for the different methods due to the different strategies to select such end-points.

In Fig. 4, we present some details on the comparison of the initial vectorization with the one provided by the active contour model. We observe that the active contour model provides a better matching of the Bézier curves and silhouette contour and that the original position of the Bézier curves end points can be shifted by the active contour model.

In Fig. 5, we illustrate the effect of the regularization parameter w_n (by default $w_n \equiv 0$). We show that when $w_n > 0$ in a Bézier curve section, the energy minimization of the active contour model produces a regularization of the Bézier curve by minimizing its length.

Silhouette	Nodes	$d(\mathcal{B}_\kappa^0, C)$	$d(\mathcal{B}_\kappa^\infty, C)$	Var. Perc.	$d(C, \mathcal{B}_\kappa^0)$	$d(C, \mathcal{B}_\kappa^\infty)$	Var. Perc.
	46	1.08	0.57	-47.33%	1.02	0.61	-40.47%
	28	1.48	0.68	-54.10%	1.46	0.68	-53.24%
	61	1.39	0.86	-37.71%	1.62	1.12	-30.75%

Silhouette	Nodes	$d(\mathcal{B}_I^0, C)$	$d(\mathcal{B}_I^\infty, C)$	Var. Perc.	$d(C, \mathcal{B}_I^0)$	$d(C, \mathcal{B}_I^\infty)$	Var. Perc.
	48	0.97	0.82	-15.46%	0.86	0.80	-7.11%
	32	0.98	0.59	-39.50%	1.09	0.59	-45.58%
	111	0.92	0.61	-34.24%	1.15	0.77	-33.17%

Silhouette	Nodes	$d(\mathcal{B}_A^0, C)$	$d(\mathcal{B}_A^\infty, C)$	Var. Perc.	$d(C, \mathcal{B}_A^0)$	$d(C, \mathcal{B}_A^\infty)$	Var. Perc.
	53	0.97	0.62	-36.76%	0.83	0.60	-27.47%
	25	1.89	1.08	-42.85%	1.70	1.00	-40.90%
	117	1.15	0.72	-37.76%	1.18	0.88	-25.66%

Table 1 From top to bottom we show the results obtained for the basic curvature method given by \mathcal{B}_κ^0 (initial guess for the active contour model) and $\mathcal{B}_\kappa^\infty$ (final result), the Inkscape software, \mathcal{B}_I^0 and \mathcal{B}_I^∞ and the Adobe Illustrator software \mathcal{B}_A^0 and \mathcal{B}_A^∞ . In each row, from left to right, we show: a snapshot of the silhouette used in the experiment, the number of nodes (end points) of the Bézier curves, the values of the distances between the curve C and the corresponding Bézier curves and the variance percentage of the distance before and after the application of the active contour model.

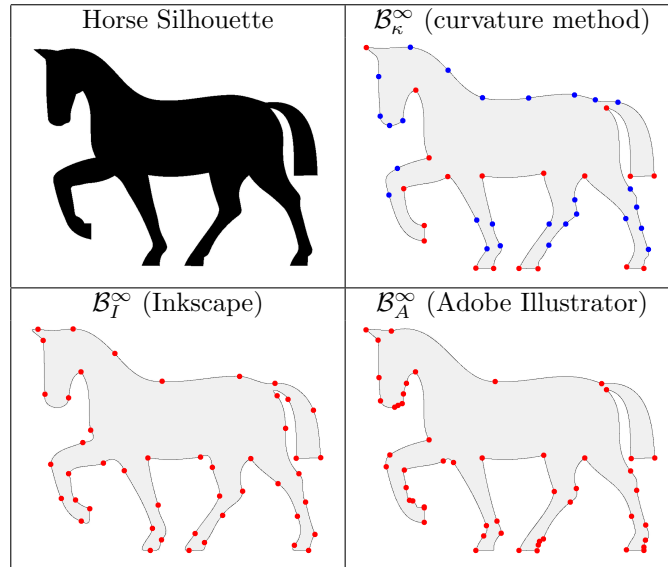


Fig. 1 Horse silhouette and the asymptotic state of the active contour models using as initial guess the vectorization provided by different methods. Blue circles represent regular points and red circles corners.

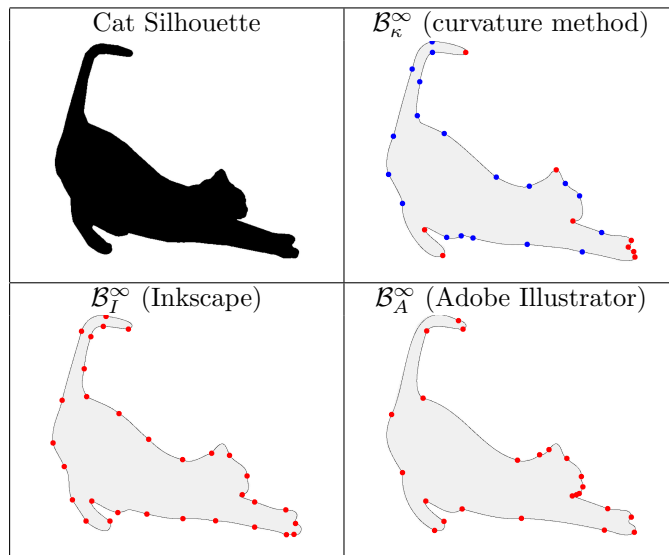


Fig. 2 Cat silhouette and the asymptotic state of the active contour models using as initial guess the vectorization provided by different methods. Blue circles represent regular points and red circles corners.

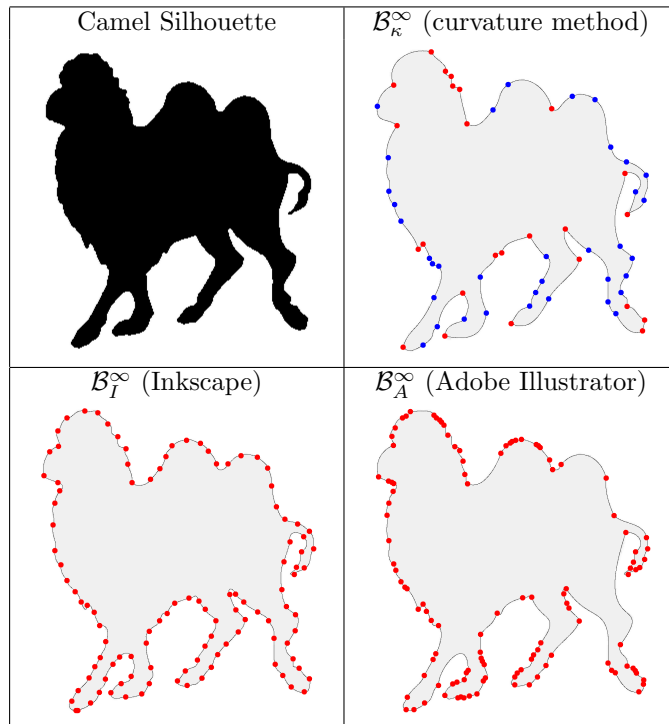


Fig. 3 Camel silhouette and the asymptotic state of the active contour models using the vectorization provided by different methods as initial guess. Blue circles represent regular points and red circles corners.

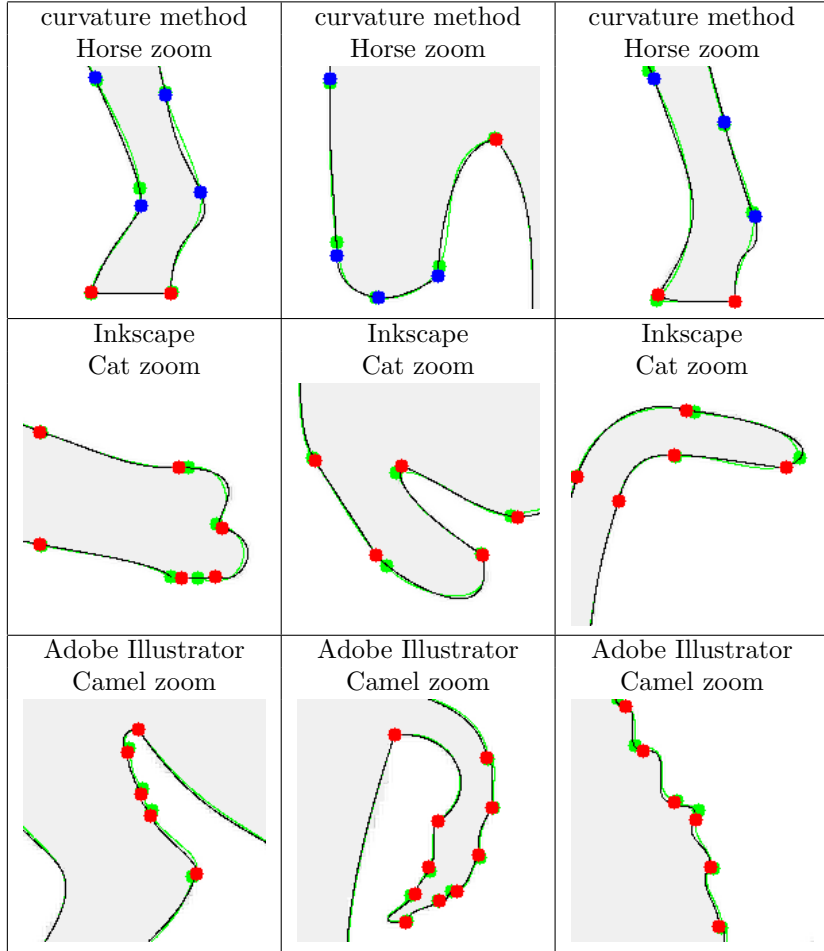


Fig. 4 We present a zoom of different parts of the silhouettes. The asymptotic state of the active contour model is represented by blue circles (regular points) or red circles (corners) with the drawing of the Bézier curves in black. The original silhouette vectorization is represented in green.

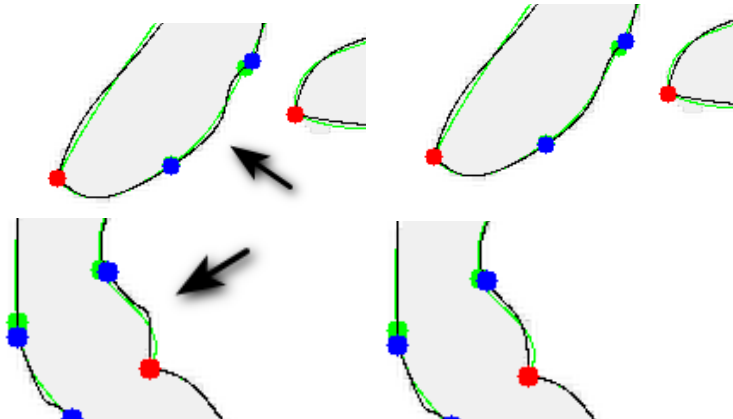


Fig. 5 On the left, we present a zoom of the vectorization of the camel silhouette using the basic curvature method with the regularization default value $w_n \equiv 0$. On the right, we present the result obtained using $w_n = 30$ as regularization parameter for the marked Bézier curve section.

6 Conclusion

Based on the geodesic active contour formulation introduced by Caselles et al. in [63], we propose an active contour model that optimizes the approximation of a curve $C(t)$ by a collection of cubic Bézier curves $\{B_n(s)\}$. By minimizing the associated energy, this model is able to optimize the location of points on $C(t)$ used as end points of the Bézier curves, the orientation of the tangent vectors in the regular points ($t_n \notin \text{Corners}$) and the parameters of the Bézier curves. We tested our method using as an initial guess the vectorization provided by a basic vectorization method based on the silhouette contour curvature and the world-class graphics software Inkscape and Adobe Illustrator. In all cases, using the proposed method, we observed a significant reduction in the distance between $C(t)$ and $\{B_n(s)\}$. The additional regularity parameters w_n included in the active contour model allow for an additional regularization of each Bézier curve section (if needed).

References

- [1] Bachmann, T.: Perception of Pixelated Images. Academic Press, (2016)
- [2] Attneave, F.: Physical determinants of the judged complexity of shapes. *Journal of experimental Psychology* **53**(4), 221 (1957)
- [3] Elder, J.H.: Are edges incomplete? *International Journal of Computer Vision* **34**(2-3), 97–122 (1999)
- [4] Torralba, A.: How many pixels make an image? *Visual neuroscience* **26**(1), 123–131 (2009)
- [5] Tian, X., Günther, T.: A survey of smooth vector graphics: Recent advances in representation, creation, rasterization and image vectorization. *IEEE Transactions on Visualization and Computer Graphics* (2022)
- [6] Dziuba, M., Jarsky, I., Efimova, V., Filchenkov, A.: Image vectorization: a review. *arXiv preprint arXiv:2306.06441* (2023)
- [7] He, Y., Kang, S.H., Alvarez, L.: Finding the skeleton of 2d shape and contours: Implementation of hamilton-jacobi skeleton. *Image Processing On Line* (2021)
- [8] He, Y., Kang, S.H., Morel, J.-M.: Silhouette vectorization by affine scale-space. *Journal of Mathematical Imaging and Vision*, 1–16 (2022)
- [9] He, Y., Kang, S.H., Morel, J.-M.: Topology- and perception-aware image vectorization. *Journal of Mathematical Imaging and Vision* **65**(6), 874–893 (2023)
- [10] Orzan, A., Bousseau, A., Winnemöller, H., Barla, P., Thollot, J., Salesin, D.: Diffusion curves: a vector representation for smooth-shaded images. *ACM Transactions on Graphics (TOG)* **27**(3), 1–8 (2008)
- [11] Hilaire, X., Tombre, K.: Robust and accurate vectorization of line drawings. *IEEE Transactions on Pattern Analysis and Machine Intelligence* **28**(6), 890–904 (2006)
- [12] Noris, G., Hornung, A., Sumner, R.W., Simmons, M., Gross, M.: Topology-driven vectorization of clean line drawings. *ACM Transactions on Graphics (TOG)* **32**(1), 1–11 (2013)
- [13] Favreau, J.-D., Lafarge, F., Bousseau, A.: Fidelity vs. simplicity: a global approach to line drawing vectorization. *ACM Transactions on Graphics (TOG)* **35**(4), 1–10 (2016)
- [14] Zhang, S.-H., Chen, T., Zhang, Y.-F., Hu, S.-M., Martin, R.R.: Vectorizing cartoon animations. *IEEE Transactions on Visualization and Computer Graphics* **15**(4), 618–629 (2009)
- [15] Yang, M., Chao, H., Zhang, C., Guo, J., Yuan, L., Sun, J.: Effective clipart image vectorization through direct optimization of bezigons. *IEEE transactions on visualization and computer graphics* **22**(2), 1063–1075 (2015)
- [16] Favreau, J.-D., Lafarge, F., Bousseau, A.: Photo2clipart: Image abstraction and vectorization using layered linear gradients. *ACM Transactions on Graphics (TOG)* **36**(6), 1–11

- (2017)
- [17] He, Y., Kang, S.H., Morel, J.-M.: Binary shape vectorization by affine scale-space. *Image Processing On Line* **13**, 22–37 (2023)
- [18] He, Y., Kang, S.H., Morel, J.-M.: Viva: a variational image vectorization algorithm on dual-primal graph pairs. In: *2023 IEEE International Conference on Image Processing (ICIP)*, pp. 1285–1289 (2023). IEEE
- [19] Reddy, P., Gharbi, M., Lukac, M., Mitra, N.J.: Im2vec: Synthesizing vector graphics without vector supervision. In: *Proceedings of the IEEE/CVF Conference on Computer Vision and Pattern Recognition*, pp. 7342–7351 (2021)
- [20] Li, T.-M., Lukáč, M., Gharbi, M., Ragan-Kelley, J.: Differentiable vector graphics rasterization for editing and learning. *ACM Transactions on Graphics (TOG)* **39**(6), 1–15 (2020)
- [21] Ferraiolo, J., Jun, F., Jackson, D.: *Scalable Vector Graphics (SVG) 1.0 Specification*. iuniverse Bloomington, (2000)
- [22] Adobe: Adobe Illustrator. <https://www.adobe.com/products/illustrator.html>
- [23] Sun, J., Liang, L., Wen, F., Shum, H.-Y.: Image vectorization using optimized gradient meshes. *ACM Transactions on Graphics (TOG)* **26**(3), 11 (2007)
- [24] Lopes, R.G., Ha, D., Eck, D., Shlens, J.: A learned representation for scalable vector graphics. In: *Proceedings of the IEEE/CVF International Conference on Computer Vision*, pp. 7930–7939 (2019)
- [25] Vinker, Y., Pajouheshgar, E., Bo, J.Y., Bachmann, R.C., Bermano, A.H., Cohen-Or, D., Zamir, A., Shamir, A.: Clipasso: Semantically-aware object sketching. *ACM Transactions on Graphics (TOG)* **41**(4), 1–11 (2022)
- [26] Ma, X., Zhou, Y., Xu, X., Sun, B., Filev, V., Orlov, N., Fu, Y., Shi, H.: Towards layer-wise image vectorization. In: *Proceedings of the IEEE/CVF Conference on Computer Vision and Pattern Recognition*, pp. 16314–16323 (2022)
- [27] Pastva, T.A.: *Bezier curve fitting*. PhD thesis, Monterey, California. Naval Postgraduate School (1998)
- [28] Selinger, P.: *Potrace : a polygon-based tracing algorithm*. (2003). <https://api.semanticscholar.org/CorpusID:1419652>
- [29] Cinque, L., Levisaldi, S., Malizia, A.: Shape description using cubic polynomial bezier curves. *Pattern Recognition Letters* **19**(9), 821–828 (1998) [https://doi.org/10.1016/S0167-8655\(98\)00069-5](https://doi.org/10.1016/S0167-8655(98)00069-5)
- [30] Plass, M., Stone, M.: Curve-fitting with piecewise parametric cubics. In: *10th Annual Conference on Computer Graphics and Interactive Techniques*, pp. 229–239 (1983)
- [31] He, Y., Kang, S.H., Morel, J.-M.: Silhouette vectorization by affine scale-space. *Journal of Mathematical Imaging and Vision* **64**, 41–56 (2022)
- [32] He, Y., Kang, S.H., Morel, J.M.: Topology- and perception-aware image vectorization. *Journal of Mathematical Imaging and Vision* **1**, 1–20 (2023)
- [33] Pavlidis, T.: Segmentation of pictures and maps through functional approximation. *Computer Graphics and Image Processing* **1**(4), 360–372 (1972)
- [34] Mumford, D.B., Shah, J.: Optimal approximations by piecewise smooth functions and associated variational problems. *Communications on pure and applied mathematics* (1989)
- [35] Morel, J.-M., Solimini, S.: *Variational Methods in Image Segmentation: with Seven Image Processing Experiments* vol. 14. Springer, (2012)

- [36] Kornprobst, G.A.P., Aubert, G.: Mathematical problems in image processing. *Applied mathematical sciences* **147** (2006)
- [37] Cai, X., Chan, R., Zeng, T.: two-stage image segmentation method using a convex variant of the mumford-shah model and thresholding. *SIAM Journal on Imaging Sciences* **6**(1), 368–390 (2013)
- [38] Pock, T., Cremers, D., Bischof, H., Chambolle, A.: An algorithm for minimizing the mumford-shah functional. In: 2009 IEEE 12th International Conference on Computer Vision, pp. 1133–1140 (2009). IEEE
- [39] Chan, T.F., Vese, L.A.: A level set algorithm for minimizing the mumford-shah functional in image processing. In: *Proceedings IEEE Workshop on Variational and Level Set Methods in Computer Vision*, pp. 161–168 (2001). IEEE
- [40] Ambrosio, L., Tortorelli, V.M.: Approximation of functional depending on jumps by elliptic functional via t-convergence. *Communications on Pure and Applied Mathematics* **43**(8), 999–1036 (1990)
- [41] Kass, M., Witkin, A., Terzopoulos, D.: Snakes: Active contour models. *International journal of computer vision* **1**(4), 321–331 (1988)
- [42] Xu, C., Prince, J.L.: Snakes, shapes, and gradient vector flow. *IEEE Transactions on image processing* **7**(3), 359–369 (1998)
- [43] Amini, A.A., Tehrani, S., Weymouth, T.E.: Using dynamic programming for minimizing the energy of active contours in the presence of hard constraints. In: [1988 Proceedings] *Second International Conference on Computer Vision*, pp. 95–99 (1988). IEEE
- [44] Bresson, X., Esedoğlu, S., Vandergheynst, P., Thiran, J.-P., Osher, S.: Fast global minimization of the active contour/snake model. *Journal of Mathematical Imaging and vision* **28**(2), 151–167 (2007)
- [45] Caselles, V., Kimmel, R., Sapiro, G.: Geodesic active contours. *International journal of computer vision* **22**, 61–79 (1997)
- [46] Cao, F.: *Geometric Curve Evolution and Image Processing*. Springer, (2003)
- [47] Miranda, M.: Caccioppoli sets. *Atti della Accademia Nazionale dei Lincei. Classe di Scienze Fisiche, Matematiche e Naturali. Rendiconti Lincei. Matematica e Applicazioni* **14**(3), 173–177 (2003)
- [48] Ambrosio, L., Morel, J.-M., Masnou, S., Caselles, V.: Connected components of sets of finite perimeter and applications to image processing. *Journal of the European Mathematical Society* **3**(1), 39–92 (2001)
- [49] Grayson, M.A.: The heat equation shrinks embedded plane curves to round points. *Journal of Differential geometry* **26**(2), 285–314 (1987)
- [50] Chou, K.-S., Zhu, X.-P.: *The Curve Shortening Problem*. Chapman and Hall/CRC, (2001)
- [51] Asada, H., Brady, M.: The curvature primal sketch. *IEEE transactions on pattern analysis and machine intelligence* (1), 2–14 (1986)
- [52] Do Carmo, M.P.: *Differential Geometry of Curves and Surfaces: Revised and Updated Second Edition*. Courier Dover Publications, (2016)
- [53] Osher, S., Sethian, J.A.: Fronts propagating with curvature-dependent speed: Algorithms based on hamilton-jacobi formulations. *Journal of computational physics* **79**(1), 12–49 (1988)
- [54] Sapiro, G., Tannenbaum, A.: Affine invariant scale-space. *International journal of computer vision* **11**(1), 25–44 (1993)
- [55] Tannenbaum, A., Sapiro, G., Olver, P.J.: Invariant geometric evolutions of surfaces and volumetric smoothing. *SIAM Journal on Applied Mathematics* **57**(1), 176–194 (1997)
- [56] Angenent, S., Sapiro, G., Tannenbaum, A.:

- On the affine heat equation for non-convex curves. *Journal of the American Mathematical Society* **11**(3), 601–634 (1998)
- [57] Moisan, L.: Affine plane curve evolution: A fully consistent scheme. *IEEE Transactions on Image Processing* **7**(3), 411–420 (1998)
- [58] He, Y., Kang, S.H., Morel, J.-M.: Accurate silhouette vectorization by affine scale-space. In: 2021 IEEE International Conference on Image Processing (ICIP), pp. 1539–1543 (2021). IEEE
- [59] He, Y., Kang, S.H., Morel, J.-M.: Vectorizing images of any size. In: 2022 IEEE International Conference on Image Processing (ICIP), pp. 816–820 (2022). IEEE
- [60] Alvarez, L., Morales, F.: Affine morphological multiscale analysis of corners and multiple junctions. *International Journal of Computer Vision* **25**, 95–107 (1997)
- [61] Alvarez, L.: Corner detection using the affine morphological scale space. In: *International Conference on Scale Space and Variational Methods in Computer Vision*, pp. 29–40 (2017). Springer
- [62] Magni, A., Mantegazza, C., Novaga, M.: Motion by curvature of planar networks ii. arXiv preprint arXiv:1301.3352 (2013)
- [63] Caselles, V., Kimmel, R., Sapiro, G.: Geodesic Active Contours. *International Journal of Computer Vision* **22**, 61–79 (1997)
- [64] Chen, Y., Tagare, H.D., Thiruvankadam, S., Huang, F., Wilson, D., Gopinath, K.S., Briggs, R.W., Geiser, E.A.: Using prior shapes in geometric active contours in a variational framework. *International Journal of Computer Vision* **50**, 315–328 (2002)
- [65] Liu, H., Chen, Y., Ho, H.P., Shi, P.: Geodesic active contours with adaptive neighboring influence. In: Duncan, J.S., Gerig, G. (eds.) *Medical Image Computing and Computer-Assisted Intervention – MICCAI 2005*, pp. 741–748. Springer, Berlin, Heidelberg (2005)
- [66] Alvarez, L.: 3D curve regularization. *Rev. Real Acad. Cienc. Exactas Fis. Nat. Ser. A-Mat* **116** (106), 1–10 (2022)
- [67] Cuenca, C., González, E., Trujillo, A., Esclarin, J., Mazorra, L., Alvarez, L., Martinez, J.A., Tahoces, P.G., Carreira, J.M.: Fast and accurate circle tracking using active contour models. *Journal of Real-Time Image Processing* **14**, 793–802 (2018)
- [68] Alvarez, L., González, E., Cuenca, C., Trujillo, A., Tahoces, P.G., Carreira, J.M.: Ellipse motion estimation using parametric snakes. *Journal of Mathematical Imaging and Vision* **60** (7), 1–10 (2018)
- [69] He, Y., Kang, S.H., Alvarez, L.: Finding the skeleton of 2d shape and contours: Implementation of hamilton-jacobi skeleton. *IPOLE Journal : Image Processing On Line* **11**, 18–36 (2021)

Appendix. A basic vectorization algorithm based on the curvature of the silhouette contour

We denote by $\mathcal{N}_r(t)$, a neighborhood in $C(t)$ of radius $r \geq 0$ defined by

$$\mathcal{N}_r(t) := \{t' \in [0, T] : |C_{t,t'}| \leq r\} \cup \{t' \in [0, T] : |C_{t',t}| \leq r\}.$$

Given a scale parameter $\sigma > 0$ we define a corneriness measure $\kappa_\sigma(C(t))$ by

$$\kappa_\sigma(C(t)) := \frac{(C(t+h_\sigma) - C(t), C(t-h'_\sigma) - C(t))}{\|C(t+h_\sigma) - C(t)\| \|C(t-h'_\sigma) - C(t)\|} + 1.$$

where (\cdot, \cdot) represents the usual dot product and $h_\sigma, h'_\sigma \geq 0$ satisfy $|C_{t,t+h_\sigma}| = |C_{t,t-h'_\sigma}| = \sigma$. This definition is explained by the remark that if $C(t)$ has a perfect corner at t of angle α , then $\kappa_\sigma(C(t)) = \cos(\alpha) + 1$. The parameter σ is also used to compute the initial tangent vector $\mathcal{T}(\alpha)$: we fix α as the orientation angle of $C'_\sigma(t)$,

where $C_\sigma(t)$ is a Gaussian convolution of $C(t)$ with standard deviation σ .

The algorithm starts by iteratively defining the set *Corners*. At each iteration we compute

$$t' := \arg \max_{t \in [0, T] - \cup_{t \in \text{Corners}} \mathcal{N}_r(t)} \kappa_\sigma(C(t)) \quad (13)$$

if $\kappa_\sigma(C(t')) \geq \kappa_{\min}$, then we include t' in *Corners* and we iterate. The threshold κ_{\min} is a fixed method parameter and $r = \text{MinLength}$. In short, *Corners* is a set of points with large enough cornerness $\kappa_\sigma(C(t))$ and separated from each other by a distance larger than *MinLength*, where *MinLength* is a parameter of the algorithm representing the minimum length allowed for $|C_{t_n, t_{n+1}}|$. Next, we iteratively introduce additional regular points. At each iteration, we first estimate $B_n(s)$ using the linear estimation obtained by minimizing (8) with the current selected points and we compute

$$\bar{x}' := \arg \max_{s, 1 \leq n \leq N} d_C(B_n(s)) \quad (14)$$

then, if $d_C(\bar{x}') > \text{MaxDist}$ we add, as regular point, the value

$$t' = \arg \min_{t \in [0, T] - \cup_{1 \leq n \leq N} \mathcal{N}_{2r}(t_n)} \|C(t) - \bar{x}'\| \quad (15)$$

and we iterate again. That is, we include regular points in locations where the Bézier curves is far from $C(t)$.

The main parameters of the algorithm are :

1. *MaxDist* : the maximum distance allowed between the Bézier curves and the original curve $C(t)$. This is the most important parameter of the algorithm and determines the number of end points of the Bézier curves. In all the experiments presented, we fix $\text{MaxDist} = 6$ which provides a few interpolation values allowing a better illustration of the performance of the proposed active contour model.
2. *MinLength* : the minimum length distance (along the curve $C(t)$) between the selected points. In all the experiments presented, we fix $\text{MinLength} = 25$.
3. σ : scale parameter used to estimate the cornerness measure and the tangent vector to $C(t)$. In all the experiments presented, we fix $\sigma = 20$.

4. κ_{\min} : the threshold value of the cornerness measure to define the set *Corners*. In all the experiments presented, we fix $\kappa_{\min} = 0.5$.